Dynamical and statistical description of multifragmentation in heavy-ion collisions

Lihua Mao (毛莉花),[1] Ning Wang (王宁),[1,2,*] and Li Ou (欧立)[1,2,†]
[1]*College of Physics and Technology, Guangxi Normal University, Guilin 541004, China*
[2]*State Key Laboratory of Theoretical Physics, Institute of Theoretical Physics, Chinese Academy of Sciences, Beijing 100190, China*
(Received 7 February 2015; published 7 April 2015)

To explore the roles of the dynamical model and statistical model in the description of multifragmentation in heavy-ion collisions at intermediate energies, the fragments charge distributions of ^{197}Au+^{197}Au at 35 MeV/u are analyzed by using the hybrid model of improved quantum molecular dynamics (ImQMD) model plus the statistical model GEMINI. We find that, the ImQMD model can well describe the charge distributions of fragments produced in central and semicentral collisions. But for the peripheral collisions of Au+Au at 35 MeV/u, the statistical model is required at the end of the ImQMD simulations for the better description of the charge distribution of fragments. By using the hybrid model of ImQMD+GEMINI, the fragment charge distribution of Au+Au at 35 MeV/u can be reproduced reasonably well. The time evolution of the excitation energies of primary fragments is simultaneously investigated.

DOI: 10.1103/PhysRevC.91.044604 PACS number(s): 24.10.Cn, 24.10.Pa, 25.70.Mn, 25.70.Pq

I. INTRODUCTION

The heavy-ion nuclear reactions at intermediate and high energies provide a unique approach to study the nuclear equation of state at high densities in terrestrial laboratories, and therefore attracted much attentions both in experimental and theoretical fields [1–8]. Because of the very short time scale in heavy-ion collisions, it is difficult to record the dynamical process of reactions by the experimental equipment. What the experiments can provide are the phase space information of various particles produced in the reactions. To know what happened during the reactions, especially before the system equilibrium, reliable dynamical approaches are crucial to extract physics from heavy-ion collision experiments. Many transport theories have been developed to explain the relevant experimental data. The models can be classified into two main categories: one-body theory and n-body theory. The popular one-body theories include the time dependent Hartree-Fock [9–11] and the Boltzmann-Vlasov (BV) approach [12–14], e.g., isospin-dependent Boltzmann-Uehling-Uhlenbeck (IBUU), relativistic BUU (RBUU), BUU by P. Danielewicz (pBUU), Giessen BUU (GiBUU), relativistic Vlasov-Uehling-Uhlenbeck (RVUU) *et al.*, in BV family. One of the popular n-body theories is the molecular dynamics (MD) approach, e.g., quantum molecular dynamics (QMD), improved QMD (ImQMD), isospin-dependent QMD (IQMD), ultrarelativistic QMD (UrQMD), antisymmetrized molecular dynamics (AMD), constrained molecular dynamics (CoMD) *et al.*, in MD family. With many efforts on the study of heavy-ion reactions, more and more observables are obtained and need to be explained by the transport model, the reliability of transport models faces a great challenge. One of the most challenging tasks for the n-body theory in nuclear physics is the description of the multifragmentation of heavy nuclei. The investigation of multifragmentation [15–20] is important for understanding the reaction mechanism in heavy-ion collisions. One-body theories are not proper tools for the investigation of many-body correlations, because the formation of fragments is beyond the scope of these models. Other kinds of theory are the statistical approaches, i.e., statistical or thermodynamical models, such as the canonical thermodynamical model (CTM) [18], statistical multifragmentation model (SMM) [19], GEMINI model [21,22], GEM2 [23,24] model, and HIVAP code [25]. The statistical approach is more appropriate to study nuclei in the equilibrium state. So the statistical approach is used to describe the spectator in peripheral heavy-ion collisions.

The n-body theory can well describe the multifragmentation process in central and semicentral heavy-ion reactions at intermediate and high energies, in which the large density fluctuations caused by compression and expansion and high excitation energies of the system play a dominant role for the formation of fragments. However, the n-body theory fails to self-consistently describe the peripheral heavy-ion collisions and spallation reactions with heavy nuclei because in these kinds of reactions the density fluctuations and excitation energies are relatively small and the fission of the composite system or heavy fragments could not be neglected. So the statistical analysis at the end of dynamical simulations is necessary and important, since the transport models only contain classical correlations, which is insufficient to correctly describe evaporation (where a realistic density of states are needed) or fission (where quantum fluctuations are essential). On the other hand, low energy reactions require a simulation with very long time. In practice it is a massive mission to simulate the reaction of a very heavy system with a very large time scale. The hybrid model by the dynamical plus statistical model is a good compromise to study this kind of subject.

In this paper, we use the ImQMD model plus the statistical model GEMINI to describe the multifragmentation process in heavy ion collisions. The paper is organized as follows. In Sec. II, we briefly introduce the model we adopted. In Sec. III, we present some calculations about the excitation energy and charge distribution of fragments in the reactions of ^{197}Au+^{197}Au at incident energies of $E = 35$ MeV/u. Finally a brief summary is given in Sec. IV.

*wangning@gxnu.edu.cn
†liou@gxnu.edu.cn

II. THEORETICAL APPROACHES

In the ImQMD model [26], as in the original QMD model [27], each nucleon is represented by a coherent state of a Gaussian wave packet:

$$\phi_i(\boldsymbol{r}) = \frac{1}{\left(2\pi\sigma_r^2\right)^{3/4}} \exp\left[-\frac{(\boldsymbol{r}-\boldsymbol{r}_i)^2}{4\sigma_r^2} + \frac{i}{\hbar}\boldsymbol{r}\cdot\boldsymbol{p}_i\right], \quad (1)$$

where $\boldsymbol{r}_i$ and $\boldsymbol{p}_i$ are the centers of the ith wave packet in the coordinate and momentum space, respectively. The one-body phase space distribution function is obtained by the Wigner transform of the wave function. The time evolution of $\boldsymbol{r}_i$ and $\boldsymbol{p}_i$ for each nucleon is governed by Hamiltonian equations of motion

$$\dot{\boldsymbol{r}}_i = \frac{\partial H}{\partial \boldsymbol{p}_i}, \quad \dot{\boldsymbol{p}}_i = -\frac{\partial H}{\partial \boldsymbol{r}_i}, \quad (2)$$

where

$$H = T + U_{\mathrm{Coul}} + U_{\mathrm{loc}}, \quad (3)$$

here, the kinetic energy $T = \sum_i \frac{\boldsymbol{p}_i^2}{2m}$, U_{Coul} is the Coulomb energy, and the local potential energy $U_{\mathrm{loc}} = \int V_{\mathrm{loc}}[\rho(\boldsymbol{r})]d\boldsymbol{r}$. V_{loc} is the nuclear potential energy density functional that is obtained by the effective Skyrme interaction, which reads

$$V_{\mathrm{loc}} = \frac{\alpha}{2}\frac{\rho^2}{\rho_0} + \frac{\beta}{\gamma+1}\frac{\rho^{\gamma+1}}{\rho_0^{\gamma}} + \frac{g_{\mathrm{sur}}}{2\rho_0}(\nabla\rho)^2 + \frac{C_{\mathrm{s}}}{2\rho_0}[\rho^2 - \kappa_{\mathrm{s}}(\nabla\rho)^2]\delta^2 + g_\tau\frac{\rho^{\eta+1}}{\rho_0^{\eta}}. \quad (4)$$

In this work, we adopt the parameter set IQ3 [28] (see Table I), which has been proposed and tested for describing the heavy-ion fusion reactions and the multifragmentation process, in the previous works [28,29].

At the end of the ImQMD calculations, clusters are recognized by a minimum spanning tree (MST) algorithm [27] widely used in the QMD calculations. In this method, the nucleons with relative momenta smaller than P_{c} and relative distances smaller than R_{c} are coalesced into the same cluster. In this work, $R_{\mathrm{c}} = 3.5$ fm and $P_{\mathrm{c}} = 300$ MeV/c are adopted. Then the total energy of each excited cluster is calculated in its rest frame and its excitation energy is obtained by subtracting the corresponding ground state energy from the total energy of the excited cluster. The information of excited cluster is input into the statistical decay model GEMINI to perform statistical decay stage calculations.

GEMINI is based on the well-known sequential-binary-decay picture that the individual compound nuclei decay through sequential binary decays of all possible modes, from the emission of nucleons and light particles through asymmetric to symmetric fission as well as the γ emission, until the resulting products are unable to undergo any further decay. The FORTRAN95 version (released on 2 May 2005) of GEMINI is used in this work. A very detailed description of the GEMINI can be found in Refs. [21,22] and references therein. The GEMINI parameters are chosen as following: The level density is taken as Grimes case B modified form (*aden_type* $= -23$), all asymmetric divisions is considered in fission mode (*imf_option* $= 2$), the particle with $Z \leqslant 5$ is treated in light particle evaporation (*Z_imf_min* $= 5$). The other parameters are taken as the default value given by example in GEMINI document.

III. RESULTS AND DISCUSSION

As the most important input of the GEMINI model, the excitation energy determines the decay process of the primary cluster formed in the dynamical stage. So the calculation of excitation energy should be checked carefully. We first prepare the two initial nuclei with their properties of the ground states being well described. The time evolutions of the binding energies and nuclear radii for a number of nuclei have been checked simultaneously. Only those individual nuclei which can remain stable for several thousand fm/c are taken to be good initial nuclei, and then are applied in the simulation of the reaction process.

Figure 1 presents the excitation energy distribution for the head-on collisions of ^{40}Ca+^{40}Ca ($E_{\mathrm{c.m.}} = 80$ MeV), ^{16}O+^{46}Ti ($E_{\mathrm{c.m.}} = 38$ MeV), and ^{16}O+^{92}Zr ($E_{\mathrm{c.m.}} = 50$ MeV), at 200 fm/c and 500 fm/c, respectively. To check the procedure of the calculation of excitation energy in the ImQMD model, the corresponding excitation energy $E_Q^* = E_{\mathrm{c.m.}} + Q_{gg}$ of the compound nuclei in heavy-ion fusion reaction is also presented for comparison. Here Q_{gg} denotes the Q value of the fusion reaction from ground state to ground state. $Q_{gg} = -14.3$, 12.3, and -3.9 MeV for ^{40}Ca+^{40}Ca, ^{16}O+^{46}Ti, and ^{16}O+^{92}Zr, respectively. The corresponding values of E_Q^* are 65.7, 50.3, and 46.1 MeV for the three reaction systems (see the dashed lines), respectively. One can see that at $t = 200$ fm/c, the projectile and target are well separated, so the excitation energies of target nuclei are distributed around zero. At $t = 500$ fm/c, the compound nuclei are generally formed and the peaks of the excitation energies distribution are located at around the corresponding E_Q^*. These tests indicate that the calculation results of excitation energies of primary fragments are reasonable.

The reactions of ^{197}Au+^{197}Au at incident energies of $E = 35$ MeV/u are simulated with the ImQMD model to investigate the multifragmentation behavior of the heavy-ion collision. First, we check the time evolutions of excitation energies per nucleon of primary fragments formed in reactions with impact parameters $b = 1$, 6, and 10 fm, respectively,

TABLE I. Parameter set IQ3 used in the ImQMD calculations.

α (MeV)	β (MeV)	γ	g_{sur} (MeV fm^2)	g_τ (MeV)	η	C_s (MeV)	κ_s (fm^2)	ρ_0 (fm^{-3})	σ_0 (fm)	σ_1 (fm)
-207	138	7/6	18.0	14.0	5/3	32.0	0.08	0.165	0.94	0.018

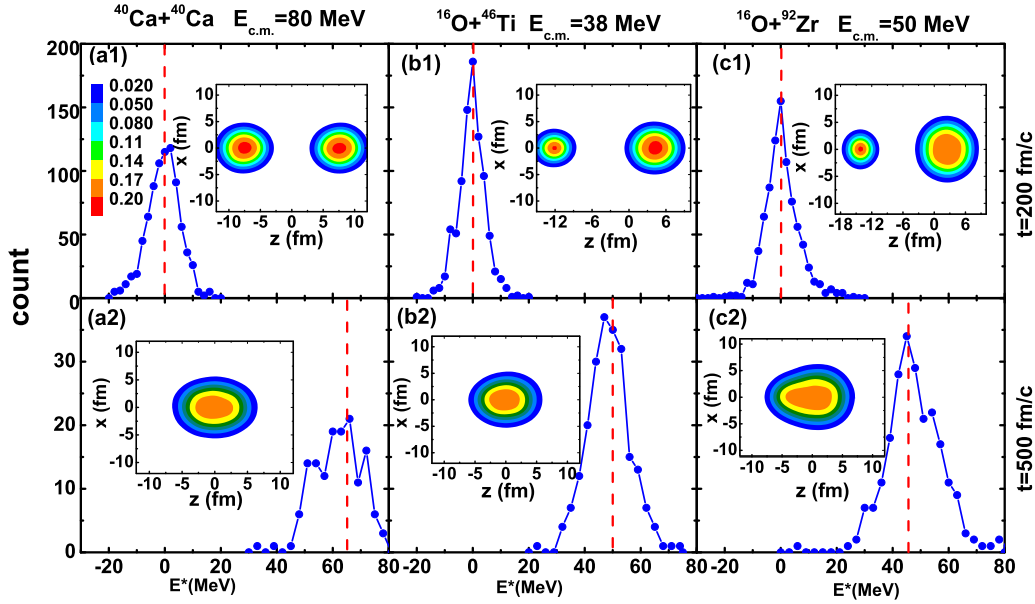

FIG. 1. (Color online) Excitation energy distribution of the largest fragments for head-on collisions of ^{40}Ca+^{40}Ca ($E_{\rm c.m.} = 80$ MeV) (left panels), ^{16}O+^{46}Ti ($E_{\rm c.m.} = 38$ MeV) (middle panels), and ^{16}O+^{92}Zr ($E_{\rm c.m.} = 50$ MeV) (right panels), at 200 fm/c (top panels) and 500 fm/c (bottom panels), respectively. The contour plot of nuclear density distribution is also presented.

as presented in Fig. 2. One can get a direct impression that with time evolution, both the excitation energies and maximum fragments become small. In the case of central and semicentral collisions, the multifragmention process can be obviously observed. The collective incident kinetic energy has transferred to the excitation energy due to the collisions between two nuclei with same size. Then the excited fragments decay by emitting free nucleons and light charged particles. So the yield of fragment with charge $Z \leqslant 10$ increase with time evolution. In the case of peripheral collisions, after $t = 500$ fm/c, there is only a few intermediate mass fragments (IMFs) yielded. The spectators with very high excitation energies are formed. With time evolution, the spectators decay by emitting free nucleons, and it only increases the yield of

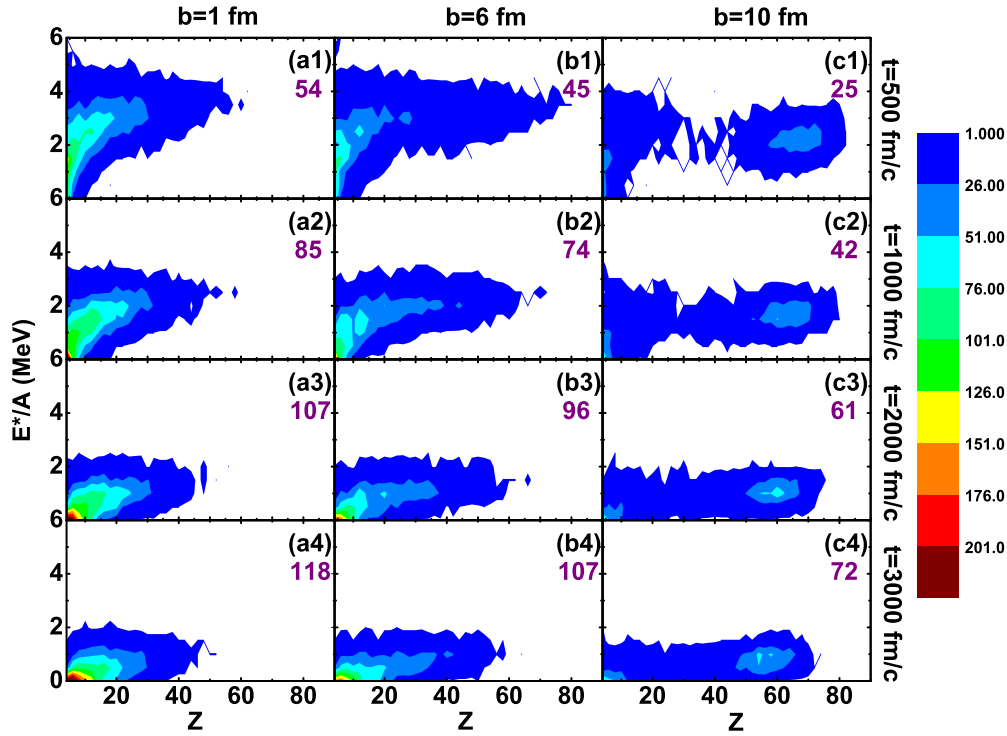

FIG. 2. (Color online) Time evolutions of the excitation energies per nucleon of primary fragments with charge number $Z \geqslant 4$ for ^{197}Au+^{197}Au at incident energy of $E = 35$ MeV/u. The average numbers of free nucleons at each event are also presented in each subfigure.

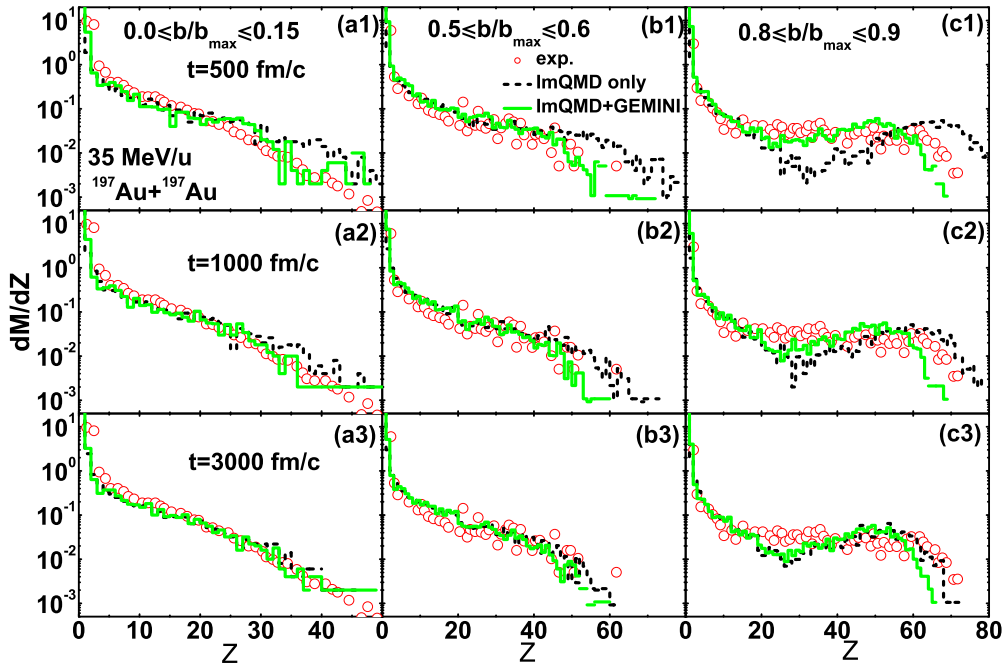

FIG. 3. (Color online) Comparison between calculations and experimental data for charge distributions of fragments in ^{197}Au+^{197}Au. The experimental data are taken from Refs. [31] for central collision and [30] for semicentral and peripheral collision, respectively.

fragment with a change around 60, but has a little contribution to the yield of IMF. Even until 3000 fm/c, there are still a certain number of fragments with high excitation energies. It indicates that the statistical description is necessary for the peripheral collisions of this reaction.

By using the hybrid model of ImQMD+GEMINI, we study the charge distribution of fragments in the reactions of ^{197}Au+^{197}Au at incident energies of $E = 35$ MeV/u. The comparison between calculations and experimental data are presented in Fig. 3. It should be noted that the incident energy is 40 MeV/u for experimental data of a central collision. We do not think there should be quite a difference in the data of 35 MeV/u. According to the experiment setup, in the case of a central collision, products in the center of mass angles between 0° and 90° are chosen to be compared with the experimental data [31]. In the semicentral and peripheral collision, products with charge up to the beam charge at $\theta_{\rm lab}$ from 3° to 23°, and products with charge up to $Z = 20$ covering the angular range from 23° to 160° are chosen to compare with experimental data [30]. One can see from the figure that, in the cases of central and semicentral collisions, the ImQMD model reproduces the experimental data reasonably well even without the statistical calculations. In the early stages of reactions, there are still some large fragments with high excitation energies. With time evolution, this results directly from the ImQMD model approach gradually to those from the ImQMD+GEMINI calculations, because the excitation energies of the fragments are exhausted by emitting particles. But in the case of peripheral collisions, the calculations without the statistical model obviously underestimate the yield of IMFs with $20 \leqslant Z \leqslant 40$. It needs a much longer time for the heavy fragments to undergo large deformation and breakup. Because of the absence of some Fermionic properties in the ImQMD model, some nucleons with high momentum will be emitted more easily and take away some excitation energies. With smaller and smaller excitation energy, the heavy fragments become difficult to break up. One can also see that, even when the simulation stops at 3000 fm/c, there is still an obvious difference between the results with and without the statistical model being involved. It means that some fragments with high excitation energies will enter the secondary decay process. From the calculations, we find that the experimental data can be well reproduced with the ImQMD+GEMINI model at switch time $t = 500$ fm/c. Finally what we want to mention is that, without any readjusting, our model can simultaneously reproduce the data taken from two different experiments with very different apparatus: INDRA+ALADIN for the central collisions, and MULTICS for the peripheral ones. It illustrates that our model has a powerful prediction ability. We note that, in the present calculations, the angular momentum of fragments is not taken into account for simplicity. In the fragmentation process, the emissions of nucleons and light particles could take away some angular momentum of heavy fragments. The neglect of angular momentum might be at the origin of the (small) discrepancy with experimental data which is still observed for the most peripheral collisions. The investigation on the influence of angular momentum of fragments is underway.

IV. SUMMARY

Multifragmentation in the intermediate heavy-ion collisions has been investigated by using the hybrid model of the improved quantum molecular dynamics model plus the statistical model GEMINI. The excitation energy of fragments in heavy-ion fusion reactions is first tested with the ImQMD model,

and the calculation results look quite reasonable. The roles of the dynamical model and statistical model in the description of the reaction mechanism are investigated by analyzing the fragments charge distribution of 35 MeV/u ^{197}Au+^{197}Au at various impact parameters. We find that, in the case of central and semicentral collisions, the calculations without the statistical calculations are in good agreement with the measured fragments charge distribution. The statistical process with nucleons and light charge particles emission can be partially represented by dynamical model. However, in the case of peripheral collisions induced by heavy nuclei, the statistical model is still necessary to describe the multifragmentation. Otherwise the IMFs yields will be underestimated due to the absence of quantum correlations in the ImQMD model. By using the hybrid model of ImQMD+GEMINI, the charge distribution of fragments in Au+Au at 35 MeV/u can be reproduced reasonably well for both central and peripheral collisions.

ACKNOWLEDGMENTS

This work has been supported by the National Natural Science Foundation of China under Grant Nos. 11005022, 11365004, 11365005, 11422548, 11275052, 11475262, 11475004 and the Open Project Program of State Key Laboratory of Theoretical Physics, Institute of Theoretical Physics, Chinese Academy of Sciences, China (No. Y4KF041CJ1).

[1] L. Shvedov, M. Colonna, and M. Di Toro, Phys. Rev. C **81**, 054605 (2010).
[2] D. Ardouin, Int. J. Mod. Phys. E **6**, 391 (1997).
[3] M. Colonna, M. Di Toro, V. Latora, and N. Colonna, Nucl. Phys. A **545**, 111 (1992).
[4] Z. Seres, F. De'ak, A. Kiss, G. Caskey *et al.*, Nucl. Phys. A **492**, 315 (1989).
[5] R. L. Watson, R. J. Maurer, B. B. Bandong, and C. Can, Lect. Notes Phys. **294**, 382 (1988).
[6] R. Planeta, F. Amorini, A. Anzalone *et al.*, Phys. Rev. C **77**, 014610 (2008).
[7] P. Staszel, Z. Majka, L. G. Sobotka *et al.*, Phys. Rev. C **63**, 064610 (2001).
[8] R. Wada, K. Hagel, J. Cibor *et al.*, Phys. Rev. C **62**, 034601 (2000).
[9] P. Bonche, S. Koonin, and J. W. Negele, Phys. Rev. C **13**, 1226 (1976).
[10] C. Golabek and C. Simenel, Phys. Rev. Lett. **103**, 042701 (2009).
[11] A. S. Umar, V. E. Oberacker, J. A. Maruhn, and P.-G. Reinhard, Eur. Phys. J. Web Conf. **17**, 09001 (2011).
[12] G. F. Bertsch, H. Kruse, and S. Das Gupta, Phys. Rev. C **29**, 673(R) (1984).
[13] B.-A. Li and D. H. E. Gross, Nucl. Phys. A **554**, 257 (1993).
[14] L. Ou and B.-A. Li, Phys. Rev. C **84**, 064605 (2011).
[15] G. F. Bertsch and S. Das Gupta, Phys. Rep. **160**, 189 (1988).
[16] A. Ono and H. Horiuchi, Prog. Part. Nucl. Phys. **53**, 501 (2004).
[17] C. Hartnack *et al.*, Eur. Phys. J. A **1**, 151 (1998).
[18] C. B. Das *et al.*, Phys. Rep. **406**, 1 (2005).
[19] J. P. Bondorf *et al.*, Phys. Rep. **257**, 133 (1995).
[20] D. H. Gross, Phys. Rep. **279**, 119 (1997).
[21] R. J. Charity, M. A. McMahan, G. J. Wozniak *et al.*, Nucl. Phys. A **483**, 371 (1988).
[22] R. J. Charity, L. G. Sobotka, Y. E. Masri *et al.*, Phys. Rev. C **63**, 024611 (2001).
[23] S. Furihata, Nucl. Instrum. Methods Phys. Res. B **171**, 251 (2000).
[24] S. Furihata and T. Nakamura, J. Nucl. Sci. Technol. Suppl. 2 **39**, 758 (2002).
[25] W. Reisdorf *et al.*, Nucl. Phys. A **444**, 154 (1985).
[26] N. Wang, Z. X. Li, and X. Z. Wu, Phys. Rev. C **65**, 064608 (2002).
[27] J. Aichelin, Phys. Rep. **202**, 233 (1991).
[28] V. Zanganeh, N. Wang, and O. N. Ghodsi, Phys. Rev. C **85**, 034601 (2012).
[29] C. Li, J. L. Tian, L. Ou, and N. Wang, Phys. Rev. C **87**, 064615 (2013).
[30] M. D'Agostino, A. S. Botvina, M. Bruno *et al.*, Nucl. Phys. A **650**, 329 (1999).
[31] F. Lavaud, E. Plagnol, G. Auger *et al.*, AIP Conf. Proc. **610**, 716 (2002).